ISSN 0915-633X

NATIONAL INSTITUTE FOR FUSION SCIENCE

True and Measured Outgassing Rates of a Vacuum Chamber with a Reversibly Absorbed Phase

K. Akaishi, M. Nakasuga and Y. Funato

(Received - Feb. 8, 2000)

NIFS-628 Mar. 2000

RESEARCH REPORT
NIFS Series

NAGOYA, JAPAN

True and Measured Outgassing Rates of a Vacuum Chamber with a Reversibly Adsorbed Phase

K. Akaishi, M. Nakasuga* and Y. Funato**

National Institute of Fusion Science
**Graduate School of Energy Science, Kyoto University*
***Suzuka National College of Technology*

Abstract

A pump down model for a vacuum chamber with a reversibly adsorbed phase is presented. The outgassing equation which predicts the variation of coverage at the wall surface of a vacuum chamber with time is derived. Then the measured and the true outgassing rates are defined. The theoretical measured outgassing rate shows only a very weak dependence for pumping speed. This prediction is opposite to the experimental result that the measured outgassing rate depends significantly on pumping speed. It is discussed that the experimental measured outgassing rate must be described as the product of the effective pumping speed and the measured pressure in the pumped chamber, in which the measured pressure is equivalent to the equilibrium pressure of the wall surface described by the equilibrium adsorption isotherm as a function of the shifted surface coverage $\theta - \Delta\theta$ by a small coverage $\Delta\theta$ from the coverage of a pumping point θ.

Key words: outgassing rate, outgassing equation, surface coverage, sticking probability, mean residence time, Temkin isotherm, 304 stainless steel chamber

Nomenclature

n: number density of gas phase molecules
σ: number of adsorbed molecules per unit area
σ_m: number of adsorbed molecules per unit area in one monolayer coverage
θ: relative coverage defined as a fraction of occupied sites with adsorbed molecules on the wall surface of a vacuum chamber, defined as

$$\theta = \sigma / \sigma_m \qquad (1)$$

V: volume of a vacuum chamber
A: area of the wall surface of a vacuum chamber
τ: mean residence time of an adsorbed molecules on a solid surface, defined as

$$\tau = \tau_0 e^{\frac{E}{RT}} \qquad (2)$$

where τ_0 is the nominal period of a vibration of an adsorbed molecule on a solid surface, E is the activation energy of desorption, R is the gas constant and T is the absolute temperature
s_0: sticking probability of a molecule on empty sites
s: effective sticking probability defined as

$$s = s_0(1-\theta) \qquad (3)$$

$n(u/4)$: arrival rate of gas phase molecules at a wall surface per unit area per unit time where u is the average velocity of molecules in gas phase
a: effective area of the pumping orifice, defined as

$$a = S/(u/4)$$

where S is the pumping speed of pumping orifice

[1] Introduction

The pump down model for a vacuum system with a reversibly adsorbed phase was reported before[1] by one of the authors. Further improvement of the earlier model is described in this paper. The improved points are: (1) the derivation procedure of the outgassing equation is reorganized; (2) the Temkin adsorption isotherm for a non-uniform surface is introduced; (3) using the Temkin adsorption isotherm, the conversion factor to transform the gas density in the non-equilibrium adsorption state to that in the equilibrium adsorption state is defined; (4) then it is shown that the change of gas density in the non-equilibrium adsorption state with time during pump down can be considered as the change of the equilibrium gas density of the wall surface of a vacuum chamber on the adsorption isotherm.

In the improved pump down model, the generation mechanism of outgassing rate in the pump down of a vacuum chamber is discussed on the $\theta - n$ plane. Then the outgassing equation which describes the variation of surface coverage with time is derived, and the measured and the true outguessing rates are defined. The outgassing equation is solved by numerical and approximate methods. Using the

solutions the dependence of measured outgassing rate on pumping speed is discussed. Finally it is discussed that the experimental result for the pumping speed dependence of outgassing rates measured by the orifice pumping method must be corrected.

[2] Pump down model

2.1 Modeling

For the modeling of the pump down of a vacuum chamber with a reversibly adsorbed phase, we assume that (1) the surface coverage in the pump down changes by less than one monolayer, (2) the adsorption of gas molecules on the wall surface is fully reversible, (3) the sticking probability is expressed by Eq. (3) for nondissociative adsorption and (4) the desorption rate is expressed as θ/τ using Eqs. (1) and (2). Then we can calculate variations of gas density and coverage with time at constant temperature from following two conservation of mass equations for gas molecules in the vacuum chamber and at the wall surface;

$$V\frac{dn}{dt} = A\sigma_m\left(-\frac{d\theta}{dt}\right) - a\left(\frac{u}{4}\right)n \qquad (4)$$

and

$$-\frac{d\theta}{dt} = \frac{\theta}{\tau} - \frac{s_0(1-\theta)}{\sigma_m}\left(\frac{u}{4}\right)n. \qquad (5)$$

For the quasi-steady state during pump down of a vacuum system, as shown in the appendix if the pumping time t after start of pump down is sufficiently longer than the time constant of pump down $V(1/a + 1/As_0)/(u/4)$, it is verified that the following condition holds;

$$V\left|\frac{dn}{dt}\right| << A\sigma_m\left|\frac{d\theta}{dt}\right|,$$

in addition by defining the pumping parameter as

$$\gamma = \frac{a}{As_0}, \qquad (7)$$

and letting

$$B = \frac{s_0(u/4)}{\sigma_m}, \qquad (8)$$

then Eqs. (4) and (5) are simplified as

$$-\frac{d\theta}{dt} = \gamma Bn \qquad (9a)$$

and

$$-\frac{d\theta}{dt} = \frac{\theta}{\tau} - (1-\theta)Bn. \qquad (9b)$$

In addition by combining Eqs. (9a) and (9b) the following relations are obtained;

$$Bn = \frac{1}{1-\theta+\gamma}\frac{\theta}{\tau} \qquad (10a)$$

or

$$\theta = (1+\gamma)\frac{Bn\tau}{1+Bn\tau} \qquad (10b)$$

and

$$-\frac{d\theta}{dt} = \frac{\gamma}{1-\theta+\gamma}\frac{\theta}{\tau}. \qquad (11)$$

Eq. (11) is the outgassing equation to predict the variation of θ with time during pump down of the vacuum chamber.

2.2. Temkin isotherm

To solve Eq. (11) by the method of variable separation, we need to express $\tau(E)$ as a function of θ. So let us first consider the relationship between surface coverage and gas density in the equilibrium adsorption state when $\gamma = 0$ and $d\theta/dt = 0$. If the gas density in the equilibrium adsorption state is n_{eq}, from Eq. (10a) and (10b) we obtain the following relations;

$$Bn_{eq} = \frac{\theta}{1-\theta}\frac{1}{\tau} \qquad (12a)$$

and

$$\theta = \frac{Bn_{eq}\tau}{1+Bn_{eq}\tau}. \qquad (12b)$$

In Eq. (12b) to express τ as a function of θ, let us introduce the Temkin isotherm for a non-uniform surface, because it is thought that the top surface of the wall of a 304 stainless steel chamber is covered with oxide layers. According to the Hayward and Trapnell procedure[2], the surface is divided into a number of uniform elements dh, on each of which the heat of adsorption is constant. Each of these elements is assumed to obey a Langmuir isotherm, so Eq. (12b) may be expressed as

$$\theta_h = \frac{Bn_{eq}\tau_0 e^{\frac{H}{RT}}}{1+Bn_{eq}\tau_0 e^{\frac{H}{RT}}}, \qquad (13)$$

and the total surface coverage θ over the whole surface is obtained by integration as

$$\theta = \sum_{h=0}^{1}\theta_h dh,$$

where H is the heat of adsorption for a non-uniform surface. If E_a and E denote the activation energies of adsorption and desorption respectively, H is given by $H = E - E_a$, and when E_a is very small compared to E, H may be treated as $H \cong E$. The Temkin isotherm assumes that E falls linearly with h

$$E = E_0 - \Delta E \cdot h \quad \text{and} \quad \Delta E = E_0 - E_1, \quad (14a)$$

where E_0 and E_1 are the activation energies of desorption at $h = 0$ and $h = 1$, the integration of Eq. (13) is expressed as

$$\theta = \int_0^1 \frac{Bn_{eq}\tau(E_0)e^{-bh}}{1 + Bn_{eq}\tau(E_0)e^{-bh}}dh, \quad (14b)$$

where

$$\tau(E_0) = \tau_0 e^{\frac{E_0}{RT}} \quad (14c)$$

and

$$b = \frac{\Delta E}{RT}. \quad (15)$$

Eq. (14b) leads

$$\theta = \frac{1}{b}\ln\left[\frac{1 + Bn_{eq}\tau(E_0)}{1 + Bn_{eq}\tau(E_0)e^{-b}}\right], \quad (16a)$$

or

$$Bn_{eq} = \frac{1}{\tau(E_0)}\left(\frac{e^{b\theta} - 1}{1 - e^{-b(1-\theta)}}\right), \quad (16b)$$

and for the range of coverage $\theta < 1$ it may be assumed that $e^{-b(1-\theta)} << 1$, Eq. (16b) simplifies to

$$Bn_{eq}\tau(E_0) = e^{b\theta} - 1. \quad (16c)$$

Eq. (16c) is the Temkin isotherm in the equilibrium adsorption state of a vacuum chamber. Using Eqs. (12b) and (16b), τ is expressed as a function of θ as follows;

$$\tau(E) = \tau(E_0)\left(\frac{\theta}{1-\theta}\right)\left(\frac{1 - e^{-b(1-\theta)}}{e^{b\theta} - 1}\right) \quad (17)$$

$$\cong \left(\frac{\theta}{1-\theta}\right)\frac{\tau(E_0)}{e^{b\theta} - 1} \equiv \tau(\theta).$$

From Eq. (17) $\tau(1)$ and $\tau(0)$ at $\theta = 1$ and $\theta = 0$ are given respectively by

$$\tau(1) \cong \tau(E_0)be^{-b} = b\tau_0 e^{\frac{E_1}{RT}}$$

$$\because \quad \lim_{\theta \to 1}\left(\frac{\theta}{1-\theta}\right)\left(\frac{1 - e^{-b(1-\theta)}}{e^{b\theta} - 1}\right) \to b$$

and

$$\tau(0) \cong \tau(E_0)/b$$

$$\because \quad \lim_{\theta \to 0}\left(\frac{\theta}{1-\theta}\right)\left(\frac{1 - e^{-b(1-\theta)}}{e^{b\theta} - 1}\right) \to 1/b.$$

2.3 Measured and true outgassing rates

If the gas densities in the equilibrium and the non-equilibrium adsorption states at the coverage θ_t are denoted as $n_{eq}(\theta_t)$, $n(\theta_t)$ and are not equal each other, i.e. $n_{eq}(\theta_t) \neq n(\theta_t)$ at $\theta = \theta_t$, because Eq. (10b) can be rewritten as

$$\theta_t = (1+\gamma)\frac{Bn(\theta_t)\tau(\theta_t)}{1 + Bn(\theta_t)\tau(\theta_t)},$$

by rewriting the term $\tau(\theta_t)$ to $n_{eq}(\theta_t)$ using Eqs. (16c) and (17), we obtain

$$\frac{n_{eq}(\theta_t)}{n(\theta_t)} = \frac{1 - \theta_t + \gamma}{1 - \theta_t} \equiv X(\theta_t). \quad (18a)$$

Here we call $X(\theta)$ as the conversion factor to express the gas density in the non-equilibrium adsorption state with that in the equilibrium adsorption state While if $n(\theta_t)$ is equivalent to the equilibrium gas density $n_{eq}(\theta_t)$ on the adsorption isotherm at a different coverage $\theta = \theta_t$, using Eq. (10b) again the same conversion factor as Eq. (18a) can be obtained as follows;

for $n(\theta_t) = n_{eq}(\theta_t)$ at $\theta_t \neq \theta_j$,

$$\theta_t = (1+\gamma)\frac{Bn_{eq}(\theta_j)\tau(\theta_t)}{1 + Bn_{eq}(\theta_j)\tau(\theta_t)} \quad \rightarrow$$

$$\frac{n_{eq}(\theta_t)}{n_{eq}(\theta_j)} = \frac{e^{b\theta_t} - 1}{e^{b\theta_j} - 1} = X(\theta_t). \quad (18b)$$

From Eq. (18a) we can confirm that if $0 < \gamma$, then $1 < X(\theta_t) \therefore n(\theta_t) < n_{eq}(\theta_t)$. From Eq. (18b) we can also show that for the approximation

$$\left(e^{b\theta_t} - 1\right)/\left(e^{b\theta_j} - 1\right) \cong e^{b(\theta_t - \theta_j)},$$

$$0 < (\ln X)/b \cong (\theta_t - \theta_j) \therefore \theta_j < \theta_t,$$

then the non-equilibrium adsorption isotherm is expressed as

$$Bn(\theta_t)\tau(E_0) \cong e^{-b(\theta_t - \theta_j)} \cdot e^{b\theta}. \quad (18c)$$

If we consider that the pump down of a vacuum chamber is started from the following initial conditions; at $t = 0$

$$\theta = \theta_t$$

and

$$n_{eq}(\theta_t) = \left[e^{b\theta_t} - 1\right]/B\tau(E_0),$$

we can depict the relationships between respective gas densities $n_{eq}(\theta_j)$, $n(\theta_t)$ and $n_{eq}(\theta_t)$ on the $\theta - n$ plane shown by Kanazawa[3]. Figure 1 shows the θ - $\log n$ diagram, where the line AE is a part of the Temkin adsorption isotherm, the line BD is a part of the non-equilibrium adsorption

C, respectively. In a transient phase just after the start of pump down, the gas density in the vacuum chamber starts to decrease from the point A to B without decrease of surface coverage, where the source term of desorption (θ/τ) does not decrease but the readsorption rate of gas molecules from the gas phase onto the wall surface decreases to compensate for the drop of gas density due to pumping. Then the source term of desorption starts to decrease from the point B to D on the line BD by releasing gas molecules so as to compensate for the non-equilibrium state between the wall surface and the gas phase. so that the decrease of surface coverage occurs from θ_t to θ_j. Because the equilibrium gas density $n_{eq}(\theta_j)$ which corresponds to the non-equilibrium gas density $n(\theta_t)$ changes from $n_{eq}(\theta_j)$ to $n_{eq}(\theta_k)$ on the line CE, the surface coverage changes from θ_j to θ_k so as to keep the equivalence $n_{eq}(\theta_j) = n(\theta_t)$ between the equilibrium and the non-equilibrium gas densities. If $\Delta\theta = \theta_j - \theta_k$ denotes the deviation of coverage from the point C to E in a time interval Δt due to pumping. the generation of outgassing rate may be expressed as the change of source term of desorption for the coverage change from the point C to E as follows;

$$-\Delta\theta = \left[\left(\frac{\theta}{\tau}\right)_j - \left(\frac{\theta}{\tau}\right)_k\right]\Delta t$$

$$= \begin{bmatrix} B(1-\theta_j)n_{eq}(\theta_j) \\ -B(1-\theta_j+\Delta\theta)n_{eq}(\theta_j-\Delta\theta) \end{bmatrix}\Delta t$$

and using Eq. (18b)

$$-\frac{\Delta\theta}{\Delta t} = \frac{(1-\theta_j)(\gamma-\Delta\theta)}{(1-\theta_j+\gamma)} Bn_{eq}(\theta_j),$$

then by taking the limit of $\Delta t \to 0$,we obtain

$$\lim_{\Delta t\to 0}\left(-\frac{\Delta\theta}{\Delta t}\right) \to -\frac{d\theta}{dt} = \frac{\gamma}{X(\theta_j)} Bn_{eq}(\theta_j).$$

As a result of that the non-equilibrium gas density $n(\theta_t)$ is expressed with the equivalent gas density $n_{eq}(\theta_j)$, the outgassing equation at the point B is given by

$$\left(-\frac{d\theta}{dt}\right)_j = \frac{\gamma B n_{eq}(\theta_j)}{X(\theta_j)}$$

$$= \left(\frac{\theta}{\tau}\right)_j - \frac{(1-\theta_j)Bn_{eq}(\theta_j)}{X(\theta_j)} \quad (19a)$$

using Eq. (16c) and by omitting the subscript j in θ_j in Eq. (19a), we obtain the following variable separation form for θ and t;

$$-\frac{d\theta}{dt} = \frac{1-\theta}{1-\theta+\gamma}\frac{\gamma(e^{b\theta}-1)}{\tau(E_0)}. \quad (19b)$$

In the derivation of the outguessing equation we should notice that adsorbed gas molecules at the section of surface coverage $\Delta\theta = \theta_t - \theta_j$ still remain on the wall surface without desorbing during the change of gas density from the point B to C. If q_m and q_t denote the measured and the true outgassing rates. from Eq. (19a) these can be defined as follows;

$$q_m = \sigma_m\left(-\frac{d\theta}{dt}\right) = \sigma_m \frac{\gamma B n_{eq}(\theta)}{X(\theta)} \quad (20)$$

and

$$q_t = \sigma_m\left(\frac{\theta}{\tau}\right) = \sigma_m Bn_{eq}(1-\theta)$$

$$= \left(\frac{1-\theta+\gamma}{\gamma}\right)q_m. \quad (21)$$

[3] Solutions of the outgassing equation

3.1 Variation of conversion factor

In the middle range of coverage when θ still changes near $\theta = 1/2$ during pumping down, the factor $\theta/(1-\theta)$ in the right hand side of Eq. (12a) can be approximated as $\theta/(1-\theta) \cong 1$. which is the assumption used to derive the simple Temkin isotherm. Then, the conversion factor of Eq. (18a) can be rewritten as

$$X(\theta) = \frac{1-\theta+\gamma}{\theta}. \quad (22)$$

Using Eq. (22). we may rewrite Eq. (19b) to

$$-\frac{d\theta}{dt} = \frac{\theta}{1-\theta+\gamma}\frac{\gamma(e^{b\theta}-1)}{\tau(E_0)}. \quad (23)$$

3.2 Numerical and approximate solutions

We attempt to solve numerically Eqs. (19b) and (23) over whole range of coverage. Figures 2 and 3 show the time evolution of $\theta(t)$ and $(-d\theta/dt)$ for the variation of γ when the initial surface

coverage and the maximum mean residence time are assumed as

$\theta_0 = 0.8$ at $t = 1$ s and $\tau(E_0) = 8\times10^6$ s.

In order to understand the outgassing behavior in a vacuum chamber with a reversibly adsorbed phase, we further attempt to solve approximately Eq. (19b) or (23) for the middle range of coverage. For the approximation

$$\left(e^{b\theta} - 1\right) \cong e^{b\theta},$$

the variable separation form of Eq. (19b) is written as

$$X(\theta)e^{-b\theta}\left(-\frac{d\theta}{dt}\right) = \frac{\gamma}{\tau(E_0)}.$$

Let us examine how the function $X(\theta)e^{-b\theta}$ changes with decrease of θ. By letting

$$F(\theta) = X(\theta)e^{-b\theta} \quad \text{and} \quad x = b(1-\theta),$$

$$F(\theta) \rightarrow F(x) = e^{-b}\left[\frac{(x+b\gamma)}{x}e^{x}\right],$$

then taking logarithm for $F(x)$

$$\ln F(x) = -b + x + \log(x+b\gamma) - \log(x).$$

the differential

$$\frac{dF}{F} = dx + \frac{dx}{x+b\gamma} - \frac{dx}{x}$$

shows that if $x > 1$ i.e. $\theta < 1-(1/b)$, dx is a dominant term, and hence the variation of $F(\theta)$ with θ is dominated by the exponential term $e^{-b\theta}$. Therefore, we may approximate the function $F(\theta)$ as for $\theta < 1-(1/b)$

$$F(\theta) = \left(\frac{1-\theta+\gamma}{1-\theta}\right)e^{-b\theta} = fe^{-\frac{\theta}{k}},$$

where k and f are constants. If the values of parameters b and γ are known, we can determine the values of k and f by the following average method[1,4]:

$$\langle 1/k - b\rangle = \int_{\theta_0}^{\theta}\left(\frac{1}{1-\theta+\gamma} - \frac{1}{1-\theta}\right)d\theta \Big/ \int_{\theta_0}^{\theta} d\theta \qquad (25a)$$

and

$$\langle f\rangle = \int_{\theta_0}^{\theta}\left[\frac{1-\theta+\gamma}{1-\theta}\right]e^{\left\langle\frac{1}{k}-b\right\rangle\theta}d\theta \Big/ \int_{\theta_0}^{\theta} d\theta. \quad (25b)$$

Similarly, we can write the function $F(\theta)$ for Eq. (23) as following,

$$F(\theta) = \left(\frac{1-\theta+\gamma}{\theta}\right)e^{-b\theta} = fe^{-\theta/k} \qquad (26)$$

for $1/b \le \theta \le 1$.

The constants $1/k$, f in Eq. (26) can be calculated as follows.

$$\langle 1/k - b\rangle = \int_{\theta_0}^{\theta}\left(\frac{1}{1-\theta+\gamma} + \frac{1}{\theta}\right)d\theta \Big/ \int_{\theta_0}^{\theta} d\theta \qquad (27a)$$

and

$$\langle f\rangle = \int_{\theta_0}^{\theta}\left(\frac{1-\theta+\gamma}{\theta}\right)e^{\left\langle\frac{1}{k}-b\right\rangle\theta}d\theta \Big/ \int_{\theta_0}^{\theta} d\theta. \quad (27b)$$

In the earlier paper [1], by assuming that the main desorbing gas in a vacuum system of a reversibly adsorbed phase is water vapor and the range of activation energy of desorption is from $E_1 = 15$ to $E_0 = 27$ kcal/mol, the value of b in Eq. (15b) was selected as $b = 20$. Table 1 and 2 show the numerically calculated values of constants $1/k$, f in the functions $F(\theta)$ of Eqs. (24) and (26) for $b = 20$ and $0.2 \le \theta \le 0.8$. When we use Eq. (24) and (26), Eqs. (19b) and (23) can be expressed as

$$-\frac{d\theta}{dt} = \frac{\gamma}{f\tau(E_0)}e^{\frac{\theta}{k}} \qquad (28a)$$

then the following solution is obtained;

$$\theta_J(t) = k\ln\left[\frac{fk\tau(E_0)}{\gamma(t+t_0)}\right], \quad (28b)$$

where t_0 is the delay time until the change of coverage reaches the quasi-steady state after the start of pump down of the vacuum chamber at the initial surface coverage θ_0 at $t = 0$, and is given by

$$t_0 = \frac{kf\tau(E_0)}{\gamma}e^{-\frac{\theta_0}{k}}. \qquad (28c)$$

By differentiating Eq. (28b) the measured outgassing rate is given by

$$q_m = \frac{\sigma_m k}{(t+t_0)}, \qquad (29)$$

where the coverage ranges are $\theta \le 1 - 1/b$ for Eq. (24) and $1/b \le \theta \le 1$ for Eq. (26).

4. Discussion

4.1 γ dependence of measured outgassing rate and gas density

In the section 2, it is assumed that the surface coverage in the pump down of a vacuum chamber changes by less than one monolayer. Therefore, we must confirm whether the theoretical outgassing rate satisfies the law of particle conservation. A simple test is to show that the time integration of $q_m(t)$ over whole pumping time does not exceed the total number of adsorbed molecules, i.e.

$$\int_0^\infty q_m(t)dt = \sigma_m\left[\theta(0)-\theta(\infty)\right] \le \sigma_m\theta(0) \quad (30)$$

for $\theta(\infty) << \theta(0) = \theta_0$.

If we refer the result of numerical calculation of the outgassing equation shown in Fig. 2 (a), it is confirmed that the integration of the coverage for pumping time up to $t = 1\times10^6$s is $\left[\theta(0)-\theta\left(t=10^6\text{s}\right)\right] \cong 0.76 < \theta_0 = 0.8$.

Thus we may say that the outgassing expression of Eq. (20) satisfies the law of particle conservation. Next let us examine the dependence of theoretical measured outgassing rate q_m on γ. Figure 4 shows q_m as a function of γ calculated with numerical solutions of Eqs. (19b) and (23) for pumping time $t = 72$ h, the initial coverage $\theta_0 = 0.8$ at $t = 1$ s and $\tau(E_0) = 8\times10^6$ s. In Fig. 4 q_m only decreases slightly with increase of γ when $1 \le \gamma$. It is also shown from the approximate solution of Eq. (29) that the theoretical measured outgassing rate is independent of γ, where the expression of q_m has only the constant k but as seen in Tables 1 and 2, it only decreases or increases slightly with increase of γ in the range of $1 < \gamma$. Accordingly, we may say that the measured outgassing rate does hardly depend on γ. If we accept the condition $(-d\theta/dt)$ = constant for the variation of γ, from Eq. (19a) we can in turn show the dependence of equilibrium gas density $n_{eq}(\theta_1)$ on γ as follows; for $(1-\theta_1) \cong 1$

$$n_{eq}(\theta_1) \cong \text{const.}\times\frac{1}{B}\left(\frac{1+\gamma}{\gamma}\right). \quad (31)$$

Eq. (31) shows that $n_{eq}(\theta_1)$ is dependent on the factor $(1+\gamma)/\gamma$. This prediction is also supported from the pumping speed dependence of pressure [4] observed in the outgassing measurement for a 304 stainless steel vacuum chamber by the orifice pumping method, in which the pressure decreased with increase of the ratio a/A in the region $a/A \le 10^{-4}$ and reached a constant value with increase of that in the region $10^{-4} \le a/A$. Therefore, from the relation of Eq. (31) we may interpret that the ultimate pressure in the pumped chamber is represented by the equilibrium pressure of the wall surface. If this interpretation is acceptable, although in the pump down of a vacuum chamber the equilibrium gas density $n_{eq}(\theta_t)$ when $\gamma = 0$ is not usually measured, we may estimate it as $n_{eq}(\theta_t) \cong (1+\gamma)n_{eq}(\theta_1)$. In relating to the change of equilibrium gas density for the variation of γ, we may also consider the relationship between true and measured outgassing rates. From Eq. (21) we obtain

$$q_m = \frac{\gamma}{1+\gamma}q_t \quad \text{for } (1-\theta) \cong 1.$$

This expression is the same as shown by Redhead [5], and shows that the true outgassing rate obeys the similar dependence of $(1+\gamma)/\gamma$ to the equilibrium gas density $n_{eq}(\theta_1)$ shown in Eq. (31). If q_{ads} denotes the readsorption rate, from Eq. (32) it is shown that $q_t = q_m + q_{ads}$ and $q_{ads} = q_m/\gamma$. Therefore, the true outguessing rate decreases with increase of γ due to the decrease of readsorption rate, and reaches the minimum $q_t \cong q_m$ when γ becomes greater than 1. The minimum $q_t \cong q_m$ means that the gas density of the pumped chamber with a large γ exceeds 1 is represented by the equilibrium gas density of the wall surface.

4.2 Comparison of experimental and theoretical measured outgassing rates

We reported before[4] that when the outgassing rates of the unbaked 304 stainless steel chamber were measured by the orifice pumping method in the range of ratio a/A from $(a/A)_{min} = 4.31\times10^{-6}$ to $(a/A)_{max} = 3.23\times10^{-3}$, the outgassing rates were dependent on the ratio a/A (i.e. pumping speed). However, this experimental result is inconsistent with the theoretical prediction for the measured outgassing rate. To explain this inconsistency, the two assumptions are possible: (1) the experimental measured outguessing rate should be expressed by Eq. (19a), because the gas density in the pumped chamber with a large γ exceeds 1 is represented by the equilibrium gas

density of the wall surface; (2) the conductance of the orifice of a large area effectively lowers. It is difficult to accept the second assumption from following experimental results. Mukugi [8] measured the outgassing rate of an unbaked stainless steel chamber by the throughput method, in which two orifices of pumping speeds of 1 and 10 l/s were used and two pressure gauges were set in the upstream and the downstream sides of orifices, and reported that the ratio $q(10)/q(1)$ of measured outguessing rates $q(10)$ and $q(1)$ with pumping speeds of 1 and 10 l/s changes in the range $2.8 < q(10)/q(1) < 3.8$ while the pump down of the test chamber is carried out for more than 720 h, and after the bakeout at 250 C° for 48 h the ratio becomes $q(10)/q(1)$=1, namely the pumping speed dependence for outgassing rate disappears. Tuzi et al.,[9] investigated dependence of ion current change of residual water vapor and hydrogen on pumping speed using a gas analyzer in a pumped chamber by the orifice pumping method, and reported that the ion current of hydrogen decreases inversely proportional to pumping speed, while the ion current of water shows the same decay curve with hydrogen in the region of small pumping speed but the slope of the decay curve become small in the region of large pumping speed. The pumping speed of 10 l/s used in the experiment by Mukugi is not so large, in addition the net pumping rates are measured because pressures between the upstream and the downstream of the orifice are measured, nevertheless it is observed that the measured outgassing rate clearly depends on pumping speed. In the experiment by Tuzi et al., because the linear decrease of the hydrogen ion current is observed in the region of large pumping speed, it is difficult to explain the pumping speed dependence for the change of ion current of water by the assumption of effective drop of conductance. Thus we comes to consider the first assumption. In our experiment the experimental measured outgassing rate $q_m^{\exp}$ was determined by Eq. (9a) as the product of the pumping parameter γ and the non-equilibrium gas density $n(\theta_t)$ (i.e. measured pressure in the pumped chamber) as follows;

$$q_m^{\exp} = \sigma_m B\gamma n(\theta_t). \qquad (33)$$

As we discussed for Eqs. (31) and (32), if the non-equilibrium gas density $n(\theta_t)$ is equivalent to the equilibrium gas density of the wall surface $n_{eq}(\theta_t)$, Eq. (33) is wrong expression, hence the pumping term must be corrected as $B\gamma \to B\gamma/(1+\gamma)$. If we use Eq. (33) without correcting the pumping term, by rewriting newly $q_m^{\exp}$ as $q_m(\text{error})$, we may express Eq. (33) using Eqs. (20) as

$$q_m(\text{error}) = X(\theta) q_m. \qquad (34)$$

Eq. (34) shows that the experimental outgassing rate $q_m(\text{error})$ is $X(\theta) \cong (1+\gamma)$ times as large as the theoretical outgassing rate q_m. Then let us demonstrate that Eq. (34) is right by comparing between the experimental outgassing rates[4] $q_m(\text{error})$ and the theoretical outgassing rates $X(\theta)q_m$ at the same pumping time $t = 72$ h for the variation of γ in the range from 10^{-4} to 100. To do this, the theoretical outgassing rates $X(\theta)q_m$ at the pumping time $t = 72$ h are first calculated with numerical solutions of Eqs. (19b) and (23) as a function of γ when $\theta_0 = 0.8$ at $t = 1$ s and $\tau(E_0) = 8\times10^6$ s are assumed. Next, to transform the experimental pumping parameter a/A to γ, we need to know the value of sticking probability s_0. Using the condition $(-d\theta/dt)$ = constant for variation of γ, we can estimate the sticking probability as following; if $q_m(i)$, $q_m(j)$ and $n_{eq}(i), n_{eq}(j)$ denote outgassing rates and gas densities at two different pumping parameters γ_i and γ_j , using the condition $q_m(i)/q_m(j) = 1$ we obtain from Eq. (20) the following relation;

$$\left(\frac{\gamma_i}{1+\gamma_i}\right) n_{eq}(i) = \left(\frac{\gamma_j}{1+\gamma_j}\right) n_{eq}(j),$$

by substituting $\gamma_i = (a/A)_i / s_0$ and $\gamma_i = (a/A)_j / s_0$ into the above equation, we can express the sticking probability s_0 as

$$s_0 = \frac{(a/A)_j \left[n_{eq}(i)/n_{eq}(j) - 1\right]}{\left[(a/A)_j/(a/A)_i - n_{eq}(i)/n_{eq}(j)\right]}. \qquad (35)$$

By substituting experimental values of ratios a/A for various orifices and measured pressures (i.e. gas densities) into Eq. (35), the average value of sticking probability is estimated to be $\langle s_0 \rangle = 6.12\times10^{-5}$. Thus, we can determine the values of γ for various ratios a/A in the experiment using the average sticking probability. Figure 5 shows the theoretical outgassing rates

$X(\theta)q_m$ and the experimental outgassing rates $q_m(\text{error})$ as a function of γ. As the figure shows a comparatively good agreement between experiment and theory-I, we can say that as long as we determine the experimental measured outgassing rate by Eq. (33), a wrong result for the pumping speed dependence of outgassing rate is drawn.

The sticking probability for an unbaked 304 stainless steel chamber is estimated to be $s_0 = 6.12 \times 10^{-5}$ but this value seems to be very small, because Tuzi et al.[6,7] have measured the sticking probability of water on 304 stainless steel chambers by pulsed-laser beam irradiation and reported that the values of s_0 were in the range from 10^{-3} to 10^{-1} depending on the history of pumping or the baking condition for the vacuum chambers. We seem that these different sticking probabilities results from the difference of measuring methods. In the pulsed-laser irradiation method, the test chamber is previously pumped down for a long time and after such long pump down it is considerable that many vacant sites on the wall surface are available for adsorption of water. In addition, because a very small amount of water is introduced to the test chamber as a pressure pulse in a time duration of a few 10 ns, the adsorption of water will occur according to Henry's law and so a rapid pressure drop will occur in the chamber. This may be a reason why the large sticking probability is measured in the transient phase after the generation of pressure pulse of water vapor in the test chamber. On the contrary, in the outgassing measurement only pressures of pumped chamber are measured as a function of pumping time. In such pumped chamber, a permitted method to estimate the sticking probability s_0 of the wall surface for residual water is to use Eq. (34) and the sticking probability is given as follows;

$$s_0(1-\theta) = \frac{a}{A}\frac{1}{\left[q_m(\text{error})/q_m - 1\right]}.$$

Taking into account that $q_m(\text{error})$ in Fig. 5 increases with increase of ratio a/A and q_m in Fig. 4 is constant, we can say from the above expression that the sticking probability decreases with increase of a/A, namely it becomes small when the chamber is pumped with a large pumping speed. This situation may be explained from the discussion made for Eq. (32). We may consider that even if the adsorption of residual water occurs on the wall surface, because the adsorption rate decreases with increase of γ, the contribution of the water adsorption to the pressure change in the chamber is very small. As a result, the very low sticking probability may be estimated.

4.3 Time dependence of solution

Tables 1 and 2 shows the values of constants $1/k$ and f in Eqs. (24) and (27). We notice that from the comparison between Tables 1 and 2, the value of f increases with γ and the values of product kb when $b = 20$ change from $1 \le kb$ to $kb \le 1$. This means that although the term kb is the power index in the time dependent-term of the outgassing rate $q \propto (1/t)^{kb}$, it changes depending on the variation of the conversion factor. In the comparison between Fig. 2 and Fig. 3 when γ is larger than 1, the solution of Eq. (19b) shows the decrease of coverage with time faster than that of Eq. (23). In addition, at the pumping time longer than about 5×10^5 s, the outgassing rate for $\gamma = 100$ in Fig. 2 starts to decrease exponentially with time but the outgassing rate for the same value of γ in Fig. 3 still decreases with a power function. This difference in time dependence may cause from the difference of terms θ and $(1-\theta)$ in the conversion factors.

For the low coverage range of $\theta \le 0.2$, the factor $\theta/(1-\theta)$ in Eq. (12a) can be approximated as $\theta/(1-\theta) \cong \theta$. Then Eq. (18a) simplifies to

$$X(\theta) \cong 1 + \gamma. \tag{36}$$

as a result, Eq. (19b) can be rewritten as for $\theta \le 0.2$

$$-\frac{d\theta}{dt} \cong \frac{\gamma}{1+\gamma}\frac{\left(e^{b\theta}-1\right)}{\tau(E_0)}. \tag{37}$$

The integration of Eq. (37) leads

$$q_m = \frac{\sigma_m}{\tau(E_0)}\left(\frac{\gamma}{1+\gamma}\right) \times \frac{1}{\beta \exp\left[\dfrac{b\gamma}{1+\gamma}\cdot\dfrac{t}{\tau(E_0)}\right] - 1}, \tag{38}$$

where β is the integration constant of Eq. (37) when $\theta = \theta_i$ at $t = 0$ and is expressed as $\beta = e^{b\theta_i}/\left(e^{b\theta_i} - 1\right)$. It is astonishing that when we calculated numerically Eq. (37) by extending the upper limit of coverage up to $\theta = 0.8$, nearly the same outgassing rates as shown in Fig. 2 were obtained. This means that for solving Eq. (19b) we are permitted to replace the conversion factor of Eq. (18a) with Eq. (36) in the broad range of coverage

without setting any limitation. Eq. (38) shows that in the low coverage range the time dependence of outgassing rate changes from the power function

$$q \propto (1/t)^{kh}$$

to the exponential function

$$q \propto \exp\left[-b\gamma t/(1+\gamma)\tau(E_0)\right].$$

Hence, the theory predicts that after the pump down of a very long time the outgassing rate decreases to zero.

5. Summary

The improvement of the earlier pump down model for an unbaked vacuum chamber is made. The main discussion points are summarized as follows;

(1) The conservation of mass equations for the surface coverage and gas density in the non-equilibrium adsorption state are constructed, and then the outagassing equation which describes the variation of surface coverage with time during pump down of a vacuum chamber is derived.

(2) To solve the outgassing equation, it is necessary to express the mean residence time as a function of surface coverage. To do this, the Temkin isotherm for a non-uniform surface is introduced.

(3) By the introduction of the Temkin isotherm, the gas density in the non-equilibrium adsorption state can be transformed to that in the equilibrium adsorption state. As a result, the generation mechanism of measured outgassing rate can be considered using the $\theta - n$ plane and the outgassing equation can be rewritten to a mathematically solvable form.

(4) Using numerical and approximate solutions of the outgassing equation, the dependence of measured outgassing rate on time and pumping speed was discussed. It is shown that the theoretical measured outgassing rate does hardly depend on pumping speed.

(5) A significant dependence of outgassing rate on pumping speed observed in the outgassing measurement of an unbaked stainless steel chamber is a mistake. Because the measured pressure p in the experiment represents the equilibrium pressure of the wall surface of the vacuum chamber, the measured outgassing rate $q_m^{\exp}$ for the test chamber should be expressed rightly as

$$q_m^{\exp} \cong \sigma_m B(p/k_B T)\left[\gamma/(1+\gamma)\right].$$

(6) It is shown that when the pressure of an unbaked vacuum chamber is measured by the orifice pumping method, using the condition $(-d\theta/dt)$= constant for a fixed pumping time the sticking probability of the vacuum chamber can be estimated.

Acknowledgments

The authors would like to thank P. A. Redhead and B. B. Dayton for invaluable comments on the preparation of the manuscript. They also wish to thank G. Horikoshi for invaluable discussion during his life time, and A. Miyahara for providing meetings to discuss our work. This work was supported in part by the grant-in-aid for science and research (B, No.11555008) from the ministry of education, science and culture of Japan

Appendix

From Eq. (20), the gas density $n(\theta)$ in the left-hand side of the inequality (6) can be given by

$$n(\theta) = \frac{X(\theta)}{B\gamma}\left|-\frac{d\theta}{dt}\right|. \qquad \text{(A1)}$$

and for the approximation $(1-\theta) \cong 1$ and $X(\theta) \cong 1+\gamma$, the time derivative of Eq. (A1) is expressed as

$$\left|\frac{dn}{dt}\right| \cong \frac{1+\gamma}{B\gamma}\left|\frac{d^2\theta}{dt^2}\right|, \qquad \text{(A2)}$$

by substituting Eq. (A2) into the inequality (6) we obtain

$$\frac{1+\gamma}{B\gamma}\left|\frac{d^2\theta}{dt^2}\right| << \frac{A\sigma_m}{V}\left|\frac{d\theta}{dt}\right|. \qquad \text{(A3)}$$

From Eq.(28b), it is shown that $|d\theta/dt| = k/t$ and $|d^2\theta/dt^2| = k/t^2$ for $t_0 < t$, thus the inequality (6) simplifies to

$$\tau_p + \tau_w << t\ , \qquad \text{(A4)}$$

where $(\tau_p + \tau_w)$ is a time constant of the exponential decay of gas density in the pump down of a vacuum system and τ_p, τ_w are expressed as

$$\tau_p = V/a(u/4) \qquad \text{(A5)}$$

and

$$\tau_w = V/As_0(u/4). \qquad \text{(A6)}$$

From the inequality (A4) we can say that because the time constant of pumping in the usual vacuum system is at most not over a few minutes, as long as the pump down for more than 30 min in a vacuum system is made, the inequality (6) is usually satisfied.

References

[1] K. Akaishi, J.Vac. Sci. Technol. A **17**, 229 (1999).

[2] D. O. Hayward and B. M. W. Trapnell, *Chemisorption* (Butterworth, London,1964), P.177.
[3] K. Kanazawa, J. Vac. Sci. Technol. A **7**, 3361(1986).
[4] K. Akaishi, Y. Kubota, O. Motojima, M. Nakasuga, T. Funato and M. Mushiaki, J. Vac. Sci. Technol. A **15**, 259 (1997), and
K. Akaishi, K. Ezaki, Y. Kubota and O. Motojima, J. Vac. Soc. Jpn. (in Japanese)**42**, 204 (1999).
[5] P. A. Redhead, J. Vac. Sci. Technol. A **14**, 2599(1996).
[6] Y. Tuzi, T. Tanaka, K. Takeuchi and Y. Saito, Vacuum. **47**, 705 (1996).
[7] Y. Tuzi, T. Tanaka, K. Takeuchi, and Y. Saito, J. Vac. Soc. Jpn. (in Japanese) **40**, 377, (1997).
[8] K. Mukugi, Abstract of the fall meeting of Japan Vac. Soc, (31 October - 1 November 1991, Tokyo), p 81.
[9] Y. Tuzi, Y. Kurokawa, and K. Takeuchi, J. Vac. Soc. Japn, **35**, 845 (1992).

Figure and table captions

Fig. 1. The change of gas density in a pumped chamber on the $\theta - \log n$ diagram.

Fig. 2. Time evolution of $\theta(t)$ and $(-d\theta/dt)$ calculated numerically with Eq. (19b) for different values of γ when $\theta_0 = 0.8$, $\tau(E_0) = 8\times10^6$s and $\sigma_m = 1$ are assumed, where (a) $\gamma = 100$, (b) $\gamma = 0.1$ and (c) $\gamma = 10^{-4}$.

Fig. 3. Time evolution of $\theta(t)$ and $(-d\theta/dt)$ calculated numerically with Eq. (23) for different values of γ when $\theta_0 = 0.8$, $\tau(E_0) = 8\times10^6$s and $\sigma_m = 1$ are assumed, where (a) $\gamma = 100$, (b) $\gamma = 0.1$ and (c) $\gamma = 10^{-4}$.

Fig. 4. Theoretical measured outgassing rates q_m as a function of γ calculated Eqs. (19b) and (23) for pumping time $t = 72$ h and the initial coverage $\theta_0 = 0.8$ at $t = 1$ s.

Fig. 5. Comparison between theory and experiment for wrong outgassing rates $q_m(\text{error})$ as a function of γ, where theory I and II show $q_m(\text{error})$ of Eq. (34) at the pumping time $t = 72$ h calculated with numerical solutions of Eq. (19b) and (23) for $\theta_0 = 0.8$ at $t = 1$ s and $\tau(E_0) = 8\times10^6$ s, and experiment shows measured outgassing rates [ref.4] at the pumping time $t = 72$ h. The pumping parameter $\gamma = a/As_0$ for the orifice pumping is calculated using the average sticking probability $\langle s_0 \rangle = 6.12\times10^{-5}$.

Table 1. Values of constants $1/k$ and f of Eq. (24) calculated with Eqs. (25 a,b) for variation of γ from 10^{-5} to 100 for $b = 20$ and $0.2 \le \theta \le 0.8$.

Table 2. Values of constants $1/k$ and f of Eq. (26) calculated with Eqs. (27a ,b) for variation of γ from 10^{-5} to 100 for $b = 20$ and $0.2 \le \theta \le 0.8$.

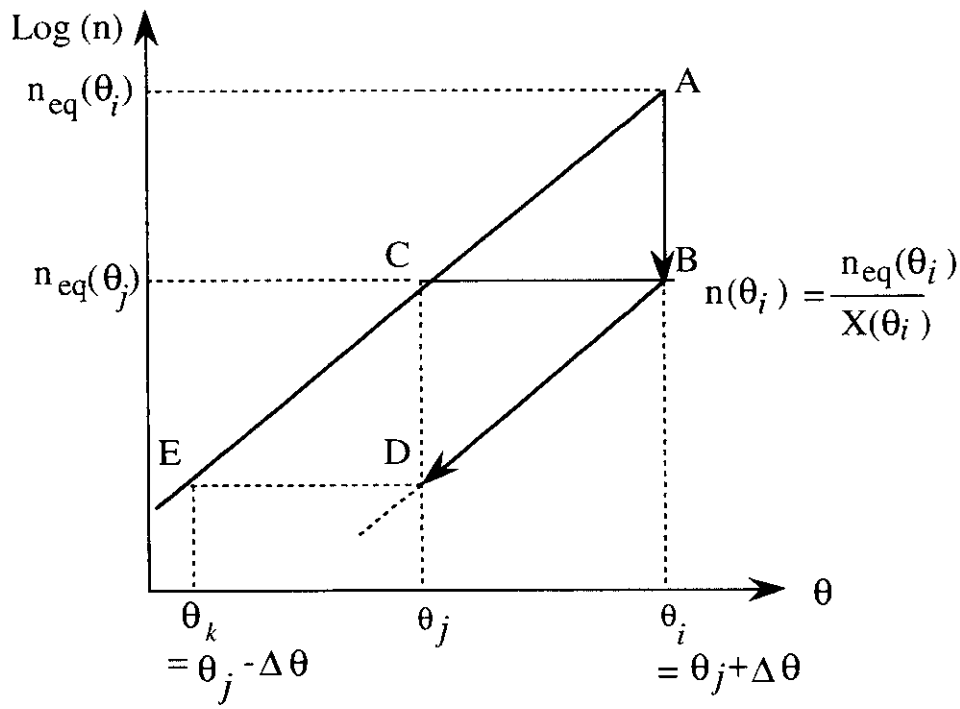

Fig. 1

Table 1.

γ	10^{2}	10^{1}	10^{0}	10^{-1}	10^{-2}	10^{-3}	10^{-4}	10^{-5}
$1/k$	17.70	17.78	18.37	19.52	19.94	19.99	20.00	20.00
f	66.47	7.246	1.370	0.935	0.985	0.998	0.998	1.00

Table 2.

γ	10^{2}	10^{1}	10^{0}	10^{-1}	10^{-2}	10^{-3}	10^{-4}	10^{-5}
$1/k$	22.30	22.26	21.63	20.48	20.06	20.01	20.00	20.00
f	628.0	62.86	6.675	1.488	1.046	1.005	1.00	1.00

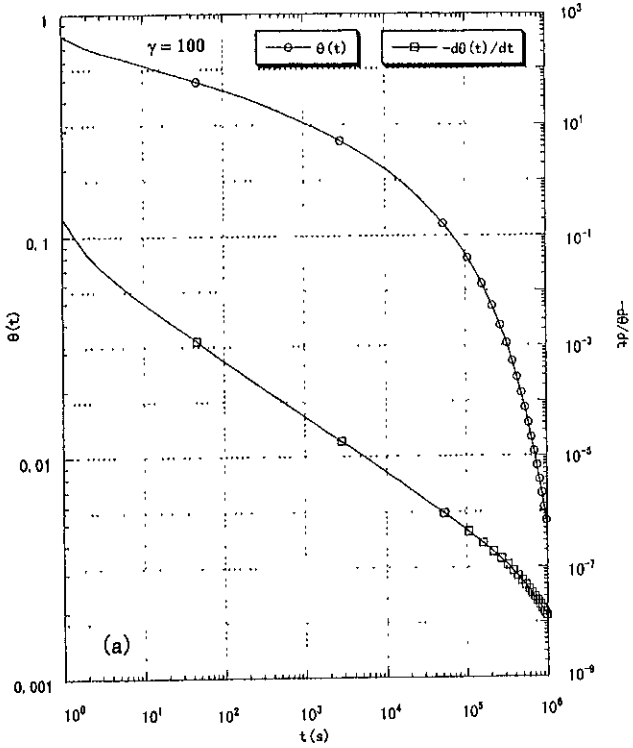

Fig. 2 (Akaishi et. al)

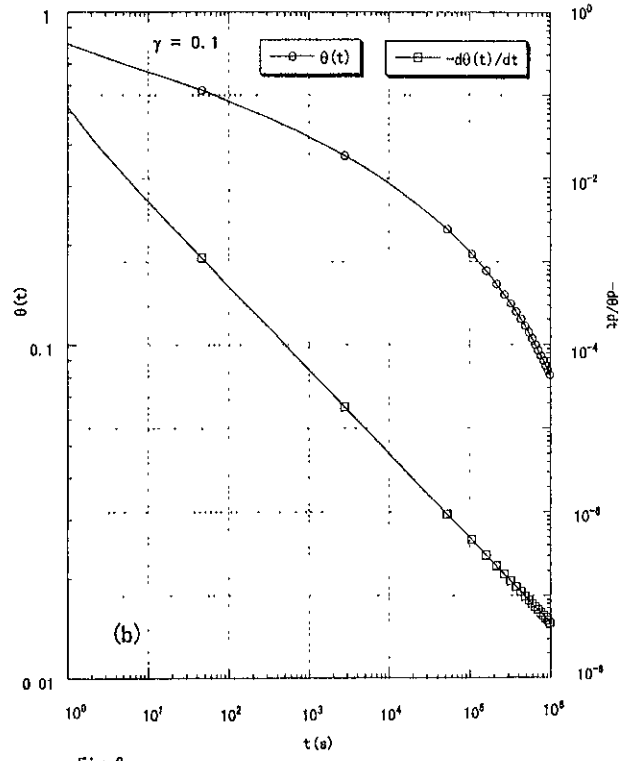

Fig. 2 (Akaishi et al)

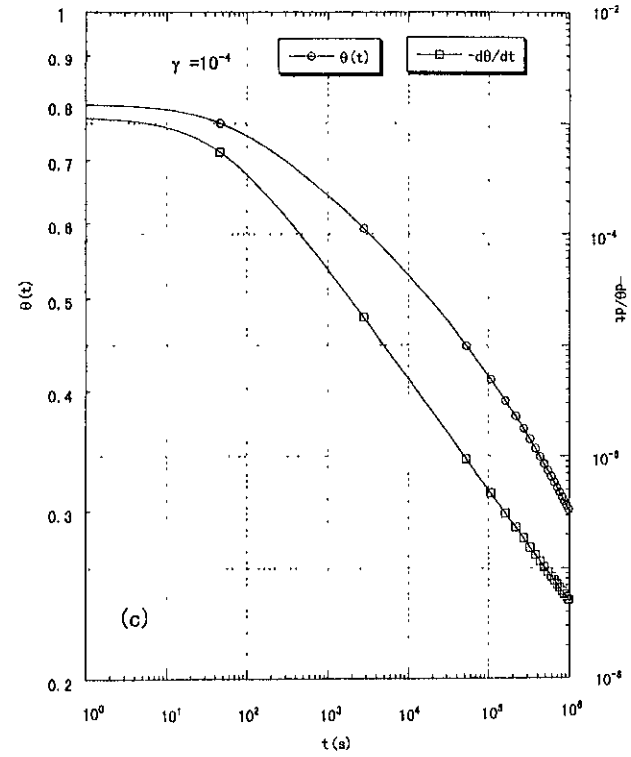

Fig. 2 (Akaishi et. al)

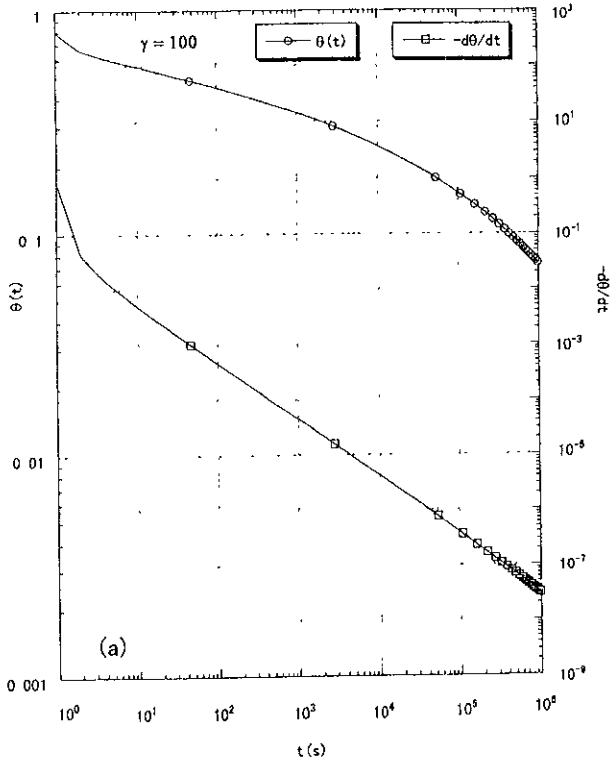

Fig 3 (Akaishi et al)

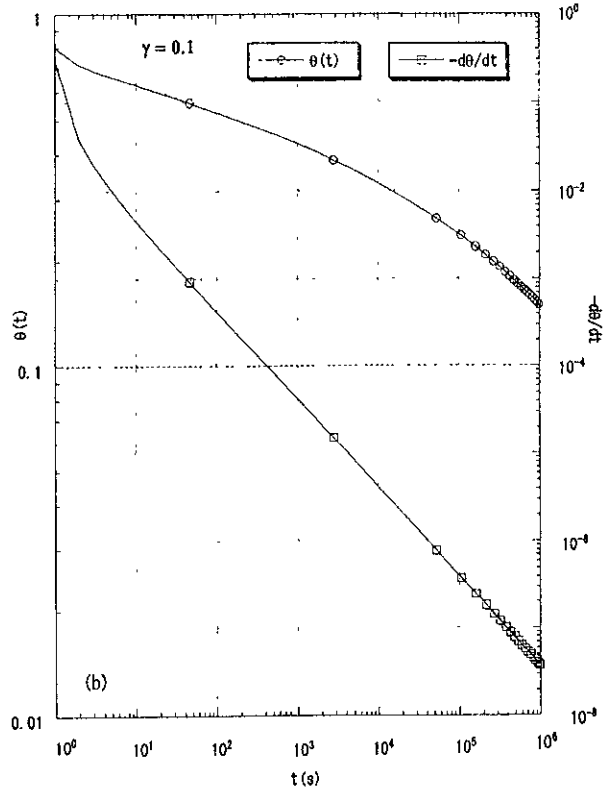

Fig. 3 (Akaishi et al.)

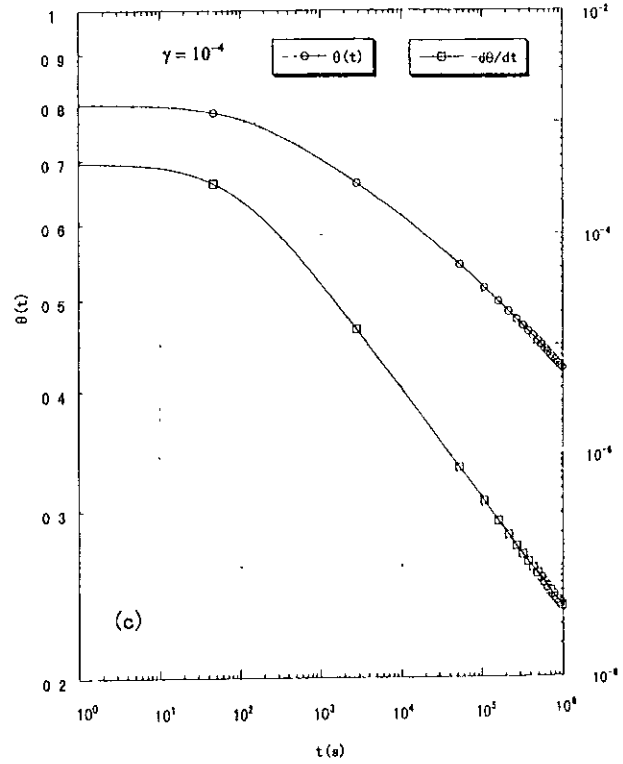

Fig 3 (Akaishi et al)

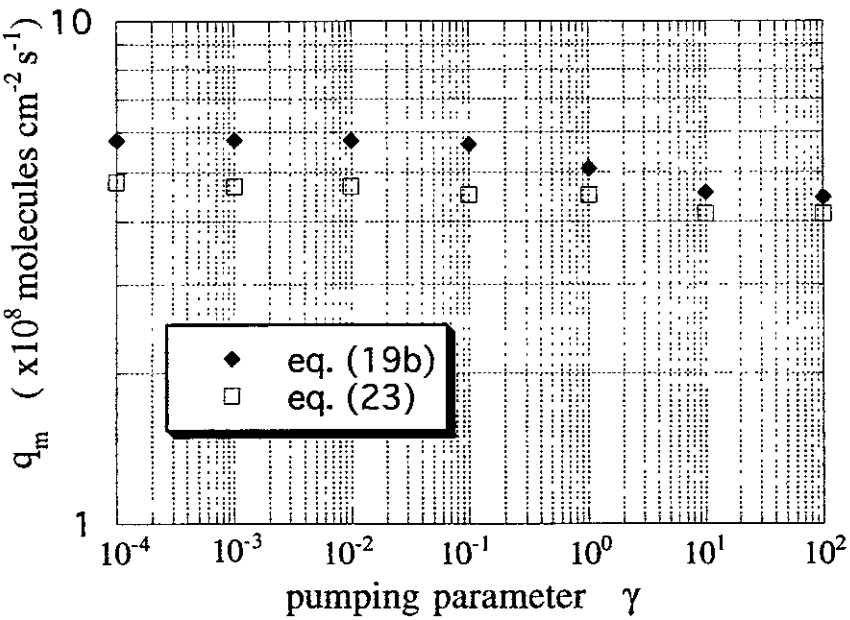
10
1
q_m (x10^8 molecules cm^{-2} s^{-1})
eq. (19b)
eq. (23)
10^{-4} 10^{-3} 10^{-2} 10^{-1} 10^0 10^1 10^2
pumping parameter γ

Fig.4

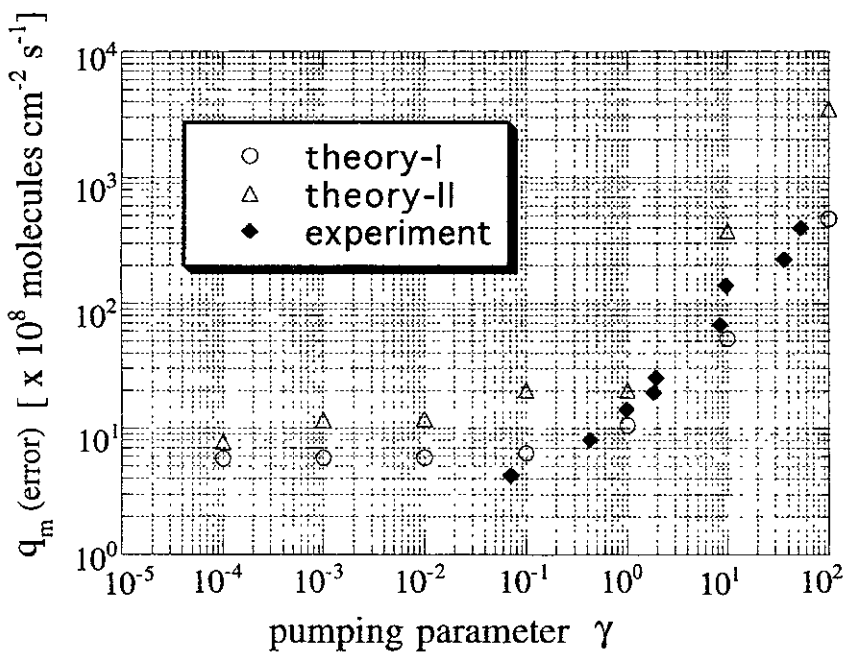
q_m (error) [x 10^8 molecules cm^{-2} s^{-1}]
10^4 10^3 10^2 10^1 10^0
theory-I
theory-II
experiment
10^{-5} 10^{-4} 10^{-3} 10^{-2} 10^{-1} 10^0 10^1 10^2
pumping parameter γ

Fig.5

Recent Issues of NIFS Series

NIFS-564 T. Watari, T. Shimozuma, Y. Takeiri, R. Kumazawa, T. Mutoh, M. Sato, O. Kaneko, K. Ohkubo, S. Kubo, H. Idei, Y. Oka, M. Osakabe, T. Seki, K. Tsumori, Y. Yoshimura, R. Akiyama, T. Kawamoto, S. Kobayashi, F. Shimpo, Y. Takita, E. Asano, S. Itoh, G. Nomura, T. Ido, M. Hamabe, M. Fujiwara, A. Iiyoshi, S. Morimoto, T. Bigelow and Y.P. Zhao,
Steady State Heating Technology Development for LHD, Oct. 1998
(IAEA-CN-69/FTP/21)

NIFS-565 A. Sagara, K.Y. Watanabe, K. Yamazaki, O. Motojima, M. Fujiwara, O. Mitarai, S. Imagawa, H. Yamanishi, H. Chikaraishi, A. Kohyama, H. Matsui, T. Muroga, T. Noda, N. Ohyabu, T. Satow, A.A. Shishkin, S. Tanaka, T. Terai and T. Uda,
LHD-Type Compact Helical Reactors, Oct. 1998
(IAEA-CN-69/FTP/03(R)

NIFS-566 N. Nakajima, J. Chen, K. Ichiguchi and M. Okamoto,
Global Mode Analysis of Ideal MHD Modes in L=2 Heliotron/Torsatron Systems, Oct. 1998
(IAEA-CN-69/THP1/08)

NIFS-567 K. Ida, M. Osakabe, K. Tanaka, T. Minami, S. Nishimura, S. Okamura, A. Fujisawa, Y. Yoshimura, S. Kubo, R. Akiyama, D.S.Darrow, H. Idei, H. Iguchi, M. Isobe, S. Kado, T. Kondo, S. Lee, K. Matsuoka, S. Morita, I. Nomura, S. Ohdachi, M. Sasao, A. Shimizu, K. Tumori, S. Takayama, M. Takechi, S. Takagi, C. Takahashi, K. Toi and T. Watari,
Transition from L Mode to High Ion Temperature Mode in CHS Heliotron/Torsatron Plasmas, Oct. 1998
(IAEA-CN-69/EX2/2)

NIFS-568 S. Okamura, K. Matsuoka, R. Akiyama, D.S. Darrow, A. Ejiri, A. Fujisawa, M. Fujiwara, M. Goto, K. Ida, H. Idei, H. Iguchi, N. Inoue, M. Isobe, K. Itoh, S. Kado, K. Khlopenkov, T. Kondo, S. Kubo, A. Lazaros, S. Lee, G. Matsunaga, T. Minami, S. Morita, S. Murakami, N. Nakajima, N. Nikai, S. Nishimura, I. Nomura, S. Ohdachi, K. Ohkuni, M. Osakabe, R. Pavlichenko, B. Peterson, R. Sakamoto, H. Sanuki, M. Sasao, A. Shimizu, Y. Shirai, S. Sudo, S. Takagi, C. Takahashi, S. Takayama, M. Takechi, K. Tanaka, K. Toi, K. Yamazaki, Y. Yoshimura and T. Watari,
Confinement Physics Study in a Small Low-Aspect-Ratio Helical Device CHS, Oct. 1998
(IAEA-CN-69/OV4/5)

NIFS-569 M.M. Skoric, T. Sato, A. Maluckov, M.S. Jovanovic,
Micro- and Macro-scale Self-organization in a Dissipative Plasma, Oct. 1998

NIFS-570 T. Hayashi, N. Mizuguchi, T-H. Watanabe, T. Sato and the Complexity Simulation Group,
Nonlinear Simulations of Internal Reconnection Event in Spherical Tokamak, Oct. 1998
(IAEA-CN-69/TH3/3)

NIFS-571 A. Iiyoshi, A. Komori, A. Ejiri, M. Emoto, H. Funaba, M. Goto, K. Ida, H. Idei, S. Inagaki, S. Kado, O. Kaneko, K. Kawahata, S. Kubo, R. Kumazawa, S. Masuzaki, T. Minami, J. Miyazawa, T. Morisaki, S. Morita, S. Murakami, S. Muto, T. Muto, Y. Nagayama, Y. Nakamura, H. Nakanishi, K. Narihara, K. Nishimura, N. Noda, T. Kobuchi, S. Ohdachi, N. Ohyabu, Y. Oka, M. Osakabe, T. Ozaki, B.J. Peterson, A. Sagara, S. Sakakibara, R. Sakamoto, H. Sasao, M. Sasao, K. Sato, M. Sato, T. Seki, T. Shimozuma, M. Shoji, H. Suzuki, Y. Takeiri, K. Tanaka, K. Toi, T. Tokuzawa, K. Tsumori, I. Yamada, H. Yamada, S. Yamaguchi, M. Yokoyama, K.Y. Watanabe, T. Watari, R. Akiyama, H. Chikaraishi, K. Haba, S. Hamaguchi, S. Iima, S. Imagawa, N. Inoue, K. Iwamoto, S. Kitagawa, Y. Kubota, J. Kodaira, R. Maekawa, T. Mito, T. Nagasaka, A. Nishimura, Y. Takita, C. Takahashi, K. Takahata, K. Yamauchi, H. Tamura, T. Tsuzuki, S. Yamada, N. Yanagi, H. Yonezu, Y. Hamada, K. Matsuoka, K. Murai, K. Ohkubo, I. Ohtake, M. Okamoto, S. Sato, T. Satow, S. Sudo, S. Tanahashi, K. Yamazaki, M. Fujiwara and O. Motojima,
An Overview of the Large Helical Device Project, Oct. 1998
(IAEA-CN-69/OV1/4)

NIFS-572 M. Fujiwara, H. Yamada, A. Ejiri, M. Emoto, H. Funaba, M. Goto, K. Ida, H. Idei, S. Inagaki, S. Kado, O. Kaneko, K. Kawahata, A. Komori, S. Kubo, R. Kumazawa, S. Masuzaki, T. Minami, J. Miyazawa, T. Morisaki, S. Morita, S. Murakami, S. Muto, T. Muto, Y. Nagayama, Y. Nakamura, H. Nakanishi, K. Narihara, K. Nishimura, N. Noda, T. Kobuchi, S. Ohdachi, N. Ohyabu, Y. Oka, M. Osakabe, T. Ozaki, B. J. Peterson, A. Sagara, S. Sakakibara, R. Sakamoto, H. Sasao, M. Sasao, K. Sato, M. Sato, T. Seki, T. Shimozuma, M. Shoji, H. Sazuki, Y. Takeiri, K. Tanaka, K. Toi, T. Tokuzawa, K. Tsumori, I. Yamada, S. Yamaguchi, M. Yokoyama, K.Y. Watanabe, T. Watari, R. Akiyama, H. Chikaraishi, K. Haba, S. Hamaguchi, M. Iima, S. Imagawa, N. Inoue, K. Iwamoto, S. Kitagawa, Y. Kubota, J. Kodaira, R. Maekawa, T. Mito, T. Nagasaka, A. Nishimura, Y. Takita, C. Takahashi, K. Takahata, K. Yamauchi, H. Tamura, T. Tsuzuki, S. Yamada, N. Yanagi, H. Yonezu, Y. Hamada, K. Matsuoka, K. Murai, K. Ohkubo, I. Ohtake, M. Okamoto, S. Sato, T. Satow, S. Sudo, S. Tanahashi, K. Yamazaki, O. Motojima and A. Iiyoshi,
Plasma Confinement Studies in LHD; Oct. 1998
(IAEA-CN-69/EX2/3)

NIFS-573 O. Motojima, K. Akaishi, H. Chikaraishi, H. Funaba, S. Hamaguchi, S. Imagawa, S. Inagaki, N. Inoue, A. Iwamoto, S. Kitagawa, A. Komori, Y. Kubota, R. Maekawa, S. Masuzaki, T. Mito, J. Miyazawa, T. Morisaki, T. Muroga, T. Nagasaka, Y. Nakmura, A. Nishimura, K. Nishimura, N. Noda, N. Ohyabu, S. Sagara, S. Sakakibara, R. Sakamoto, S. Satoh, T. Satow, M. Shoji, H. Suzuki, K. Takahata, H. Tamura, K. Watanabe, H. Yamada, S. Yamada, S. Yamaguchi, K. Yamazaki, N. Yanagi, T. Baba, H. Hayashi, M. Iima, T. Inoue, S. Kato, T. Kato, T. Kondo, S. Moriuchi, H. Ogawa, I. Ohtake, K. Ooba, H. Sekiguchi, N. Suzuki, S. Takami, Y. Taniguchi, T. Tsuzuki, N. Yamamoto, K. Yasui, H. Yonezu, M. Fujiwara and A. Iiyoshi,
Progress Summary of LHD Engineering Design and Construction; Oct. 1998
(IAEA-CN-69/FT2/1)

NIFS-574 K. Toi, M. Takechi, S. Takagi, G. Matsunaga, M. Isobe, T. Kondo, M. Sasao, D.S. Darrow, K. Ohkuni, S. Ohdachi, R. Akiyama, A. Fujisawa, M. Gotoh, H. Idei, K. Ida, H. Iguchi, S. Kado, M. Kojima, S. Kubo, S. Lee, K. Matsuoka, T. Minami, S. Morita, N. Nikai, S. Nishimura, S. Okamura, M. Osakabe, A. Shimizu, Y. Shirai, C. Takahashi, K. Tanaka, T. Watari and Y. Yoshimura,

Global MHD Modes Excited by Energetic Ions in Heliotron/Torsatron Plasmas; Oct. 1998
(IAEA-CN-69/EXP1/19)

NIFS-575 Y. Hamada, A. Nishizawa, Y. Kawasumi, A. Fujisawa, M. Kojima, K. Narihara, K. Ida, A. Ejiri, S. Ohdachi, K. Kawahata, K. Toi, K. Sato, T. Seki, H. Iguchi, K. Adachi, S. Hidekuma, S.Hirokura, K. Iwasaki, T. Ido, R. Kumazawa, H. Kuramoto, T. Minami, L. Nomura, M. Sasao, K.N. Sato, T. Tsuzuki, I. Yamada and T. Watari,
Potential Turbulence in Tokamak Plasmas; Oct. 1998
(IAEA-CN-69/EXP2/14)

NIFS-576 S. Murakami, U. Gasparino, H. Idei, S. Kubo, H. Maassberg, N. Marushchenko, N. Nakajima, M. Romé and M. Okamoto,
5D Simulation Study of Suprathermal Electron Transport in Non-Axisymmetric Plasmas; Oct. 1998
(IAEA-CN-69/THP1/01)

NIFS-577 S. Fujiwara and T. Sato,
Molecular Dynamics Simulation of Structure Formation of Short Chain Molecules; Nov. 1998

NIFS-578 T. Yamagishi,
Eigenfunctions for Vlasov Equation in Multi-species Plasmas Nov. 1998

NIFS-579 M. Tanaka, A. Yu Grosberg and T. Tanaka,
Molecular Dynamics of Strongly-Coupled Multichain Coulomb Polymers in Pure and Salt Aqueous Solutions; Nov. 1998

NIFS-580 J. Chen, N. Nakajima and M. Okamoto,
Global Mode Analysis of Ideal MHD Modes in a Heliotron/Torsatron System: I. Mercier-unstable Equilibria, Dec. 1998

NIFS-581 M. Tanaka, A. Yu Grosberg and T. Tanaka,
Comparison of Multichain Coulomb Polymers in Isolated and Periodic Systems: Molecular Dynamics Study; Jan. 1999

NIFS-582 V.S. Chan and S. Murakami,
Self-Consistent Electric Field Effect on Electron Transport of ECH Plasmas; Feb. 1999

NIFS-583 M. Yokoyama, N. Nakajima, M. Okamoto, Y. Nakamura and M. Wakatani,
Roles of Bumpy Field on Collisionless Particle Confinement in Helical-Axis Heliotrons; Feb. 1999

NIFS-584 T.-H. Watanabe, T. Hayashi, T. Sato, M. Yamada and H. Ji,
Modeling of Magnetic Island Formation in Magnetic Reconnection Experiment; Feb. 1999

NIFS-585 R. Kumazawa, T. Mutoh, T. Seki, F. Shinpo, G. Nomura, T. Ido, T. Watari, Jean-Marie Noterdaeme and Yangping Zhao,
Liquid Stub Tuner for Ion Cyclotron Heating; Mar. 1999

NIFS-586 A. Sagara, M. Iima, S. Inagaki, N. Inoue, H. Suzuki, K. Tsuzuki, S. Masuzaki, J. Miyazawa, S. Morita, Y. Nakamura, N. Noda, B. Peterson, S. Sakakibara, T. Shimozuma, H. Yamada, K. Akaishi, H. Chikaraishi, H. Funaba, O. Kaneko, K. Kawahata, A. Komori, N. Ohyabu, O. Motojima, LHD Exp. Group 1, LHD Exp. Group 2,
Wall Conditioning at the Starting Phase of LHD, Mar. 1999

NIFS-587 T. Nakamura and T. Yabe,
Cubic Interpolated Propagation Scheme for Solving the Hyper-Dimensional Vlasov-Poisson Equation in Phase Space; Mar. 1999

NIFS-588 W.X. Wnag, N. Nakajima, S. Murakami and M. Okamoto,
An Accurate δf Method for Neoclassical Transport Calculation; Mar. 1999

NIFS-589 K. Kishida, K. Araki, S. Kishiba and K. Suzuki,
Local or Nonlocal? Orthonormal Divergence-free Wavelet Analysis of Nonlinear Interactions in Turbulence; Mar. 1999

NIFS-590 K. Araki, K. Suzuki, K. Kishida and S. Kishiba,
Multiresolution Approximation of the Vector Fields on T^3; Mar. 1999

NIFS-591 K. Yamazaki, H. Yamada, K.Y Watanabe, K. Nishimura, S. Yamaguchi, H. Nakanishi, A. Komori, H. Suzuki, T. Mito, H. Chikaraishi, K. Murai, O. Motojima and the LHD Group,
Overview of the Large Helical Device (LHD) Control System and Its First Operation; Apr. 1999

NIFS-592 T Takahashi and Y Nakao,
Thermonuclear Reactivity of D-T Fusion Plasma with Spin-Polarized Fuel, Apr 1999

NIFS-593 H Sugama,
Damping of Toroidal Ion Temperature Gradient Modes, Apr 1999

NIFS-594 Xiaodong Li,
Analysis of Crowbar Action of High Voltage DC Power Supply in the LHD ICRF System, Apr 1999

NIFS-595 K Nishimura, R Horiuchi and T Sato,
Drift-kink Instability Induced by Beam Ions in Field-reversed Configurations; Apr 1999

NIFS-596 Y Suzuki, T-H. Watanabe, T Sato and T Hayashi,
Three-dimensional Simulation Study of Compact Toroid Plasmoid Injection into Magnetized Plasmas; Apr 1999

NIFS-597 H Sanuki, K Itoh, M. Yokoyama, A Fujisawa, K Ida, S Toda, S-I. Itoh, M Yagi and A Fukuyama,
Possibility of Internal Transport Barrier Formation and Electric Field Bifurcation in LHD Plasma, May 1999

NIFS-598 S Nakazawa, N. Nakajima, M. Okamoto and N. Ohyabu,
One Dimensional Simulation on Stability of Detached Plasma in a Tokamak Divertor, June 1999

NIFS-599 S Murakami, N Nakajima, M Okamoto and J Nhrenberg,
Effect of Energetic Ion Loss on ICRF Heating Efficiency and Energy Confinement Time in Heliotrons, June 1999

NIFS-600 R Horiuchi and T. Sato,
Three-Dimensional Particle Simulation of Plasma Instabilities and Collisionless Reconnection in a Current Sheet;, June 1999

NIFS-601 W Wang, M Okamoto, N Nakajima and S Murakami,
Collisional Transport in a Plasma with Steep Gradients; June 1999

NIFS-602 T. Mutoh, R Kumazawa, T. Saki, K Saito, F Simpo, G Nomura, T. Watari, X Jikang, G Cattanei, H Okada, K Ohkubo, M Sato, S Kubo, T. Shimozuma, H. Idei, Y. Yoshimura, O. Kaneko, Y. Takeiri, M Osakabe, Y Oka, K Tsumori, A Komori, H. Yamada, K Watanabe, S Sakakibara, M Shoji, R Sakamoto, S Inagaki, J. Miyazawa, S. Morita, K Tanaka, B.J Peterson, S Murakami, T Minami, S Ohdachi, S Kado, K Narihara, H Sasao, H Suzuki, K Kawahata, N Ohyabu, Y Nakamura, H. Funaba, S. Masuzaki, S Muto, K Sato, T. Morisaki, S Sudo, Y. Nagayama, T. Watanabe, M Sasao, K. Ida, N. Noda, K Yamazaki, K Akaishi, A Sagara, K Nishimura, T Ozaki, K Toi, O Motojima, M Fujiwara, A Iiyoshi and LHD Exp. Group 1 and 2,
First ICRF Heating Experiment in the Large Helical Device; July 1999

NIFS-603 P C. de Vries, Y. Nagayama, K Kawahata, S Inagaki, H Sasao and K Nagasaki,
Polarization of Electron Cyclotron Emission Spectra in LHD; July 1999

NIFS-604 W Wang, N Nakajima, M Okamoto and S Murakami,
δf Simulation of Ion Neoclassical Transport; July 1999

NIFS-605 T Hayashi, N Mizuguchi, T Sato and the Complexity Simulation Group,
Numerical Simulation of Internal Reconnection Event in Spherical Tokamak, July 1999

NIFS-606 M Okamoto, N Nakajima and W. Wang,
On the Two Weighting Scheme for δf Collisional Transport Simulation; Aug. 1999

NIFS-607 O Motojima, A.A. Shishkin, S Inagaki, K Y Watanabe,
Possible Control Scenario of Radial Electric Field by Loss-Cone-Particle Injection into Helical Device, Aug 1999

NIFS-608 R Tanaka, T. Nakamura and T Yabe,
Constructing Exactly Conservative Scheme in Non-conservative Form, Aug 1999

NIFS-609 H Sugama,
Gyrokinetic Field Theory, Aug. 1999

NIFS-610 M Takechi, G Matsunaga, S Takagi, K.Ohkuni, K Toi, M Osakabe, M Isobe, S Okamura, K Matsuoka, A Fujisawa, H Iguchi, S Lee, T Minami, K Tanaka, Y Yoshimura and CHS Group,

Core Localized Toroidal Alfven Eigenmodes Destabilized By Energetic Ions in the CHS Heliotron/Torsatron, Sep. 1999

NIFS-611 K. Ichiguchi,
MHD Equilibrium and Stability in Heliotron Plasmas; Sep. 1999

NIFS-612 Y. Sato, M. Yokoyama, M. Wakatani and V. D. Pusovitov,
Complete Suppression of Pfirsch-Schluter Current in a Toroidal l=3 Stellarator; Oct. 1999

NIFS-613 S. Wang, H. Sanuki and H. Sugama,
Reduced Drift Kinetic Equation for Neoclassical Transport of Helical Plasmas in Ultra-low Collisionality Regime; Oct. 1999

NIFS-614 J. Miyazawa, H. Yamada, K. Yasui, S. Kato, N. Fukumoto, M. Nagata and T. Uyama,
Design of Spheromak Injector Using Conical Accelerator for Large Helical Device, Nov. 1999

NIFS-615 M. Uchida, A. Fukuyama, K. Itoh, S.-I. Itoh and M. Yagi,
Analysis of Current Diffusive Ballooning Mode in Tokamaks; Dec. 1999

NIFS-616 M. Tanaka, A.Yu. Grosberg and T. Tanaka,
Condensation and Swelling Behavior of Randomly Charged Multichain Polymers by Molecular Dynamics Simulations; Dec. 1999

NIFS-617 S. Goto and S. Kida,
Sparseness of Nonlinear Coupling; Dec. 1999

NIFS-618 M.M. Skoric, T. Sato, A. Maluckov and M.S. Jovanovic,
Complexity in Laser Plasma Instabilities Dec. 1999

NIFS-619 T.-H. Watanabe, H. Sugama and T. Sato,
Non-dissipative Kinetic Simulation and Analytical Solution of Three-mode Equations of Ion Temperature Gradient Instability; Dec. 1999

NIFS-620 Y. Oka, Y. Takeiri, Yu.I.Belchenko, M. Hamabe, O. Kaneko, K. Tsumori, M. Osakabe, E. Asano, T. Kawamoto, R. Akiyama,
Optimization of Cs Deposition in the 1/3 Scale Hydrogen Negative Ion Source for LHD-NBI System ; Dec. 1999

NIFS-621 Yu.I. Belchenko, Y. Oka, O. Kaneko, Y. Takeiri, A. Krivenko, M. Osakabe, K. Tsumori, E. Asano, T. Kawamoto, R. Akiyama,
Recovery of Cesium in the Hydrogen Negative Ion Sources; Dec. 1999

NIFS-622 Y. Oka, O. Kaneko, K. Tsumori, Y. Takeiri, M. Osakabe, T. Kawamoto, E. Asano, and R. Akiyama,
H- Ion Source Using a Localized Virtual Magnetic Filter in the Plasma Electrode: Type I LV Magnetic Filter: Dec. 1999

NIFS-623 M. Tanaka, S. Kida, S. Yanase and G. Kawahara,
Zero-absolute-vorticity State in a Rotating Turbulent Shear Flow; Jan. 2000

NIFS-624 F. Leuterer, S. Kubo,
Electron Cyclotron Current Drive at $\omega \approx \omega_c$ with X-mode Launched from the Low Field Side; Feb. 2000

NIFS-625 K. Nishimura,
Wakefield of a Charged Particulate Influenced by Emission Process of Secondary Electrons; Mar. 2000

NIFS-626 K. Itoh, M. Yagi, S.-I. Itoh, A. Fukuyama,
On Turbulent Transport in Burning Plasmas, Mar. 2000

NIFS-627 K. Itoh, S.-I. Itoh, L. Giannone,
Modelling of Density Limit Phenomena in Toroidal Helical Plasmas; Mar. 2000

NIFS-628 K. Akaishi, M. Nakasuga and Y. Funato,
True and Measured Outgassing Rates of a Vacuum Chamber with a Reversibly Absorbed Phase; Mar. 2000